Surface-Enhanced Raman Scattering Based Vibrational Stark Effect as a Spatial Probe of Interfacial Electric Fields in the Diffuse Double Layer

Vanessa Oklejas, Christopher Sjostrom, and Joel M. Harris*

Department of Chemistry, University of Utah, 315 South 1400 East, Salt Lake City, Utah 84112-0850

Received: February 24, 2003

Potential-dependent surface-enhanced Raman scattering (SERS) spectra of the nitrile stretching mode were acquired from a series of monolayers composed of alkanethiols ($HS(CH_2)_xCH_3$, where $6 \leq x \leq 10$) and mercaptododecanenitrile ($HS(CH_2)_{11}CN$). These spectra were used to investigate the diffuse double layer at a silver electrode interface modified with mixed self-assembled monolayers (SAMs). The alkanethiol species acts to dilute the nitrile-terminated thiol to isolate the nitrile reporter group within the diffuse double-layer region. Nitrile groups co-immobilized with shorter diluent alkanethiol chains are placed more deeply into the diffuse double layer (relative to the methyl terminus of the surrounding alkanethiol). Interfacial electric fields, measured using observed Stark tuning rates of the nitrile stretching frequency, were examined as a function of SAM composition to map the structure of the diffuse double-layer region versus distance from the SAM/solution interface. The trends in the experimental data are largely consistent with Gouy−Chapman theory, in which Stark tuning rates, and the interfacial electric fields from which they originate, depend on both distance of the probe from the electrode surface and the ionic strength of the aqueous phase. For measurements at the highest ionic strengths, the experimentally observed double layer appeared to extend further into solution than predicted by Guoy-Chapman theory, which is consistent with the finite size of hydrated ions and theoretical predictions of the effect of a hydrophobic interface on the structure of the adjacent water layer. The results demonstrate the ability of this spectroelectrochemical experiment to characterize diffuse double-layer structure at electrochemical interfaces on a subnanometer distance scale.

Introduction

The orientation and concentration of solute molecules and electrolyte ions in the region immediately adjacent to the metal surface, i.e., the diffuse double-layer region, assumes an important role in electrochemical processes. The structure of the diffuse double layer, which determines how applied potential decays as it propagates from a charged metal surface into solution, can affect the rates of electrode processes (e.g., adsorption and electron-transfer) and, therefore, influences the kinetics of electrochemical reactions.[1] Accordingly, detailed understanding of diffuse double-layer structure can contribute insight into electrochemical processes dependent on interfacial electron-transfer (e.g., metal corrosion, electroanalytical sensor performance, battery and fuel cell operation, synthetic electrochemistry).[2]

Most investigations of diffuse double-layer structure rely upon measurement of interfacial electric (E) fields, or associated electrostatic forces.[3,4] Large interfacial E fields are the direct result of the formation of the diffuse double layer, where discrete, mobile ions organize at the metal surface in response to the presence of excess surface charge. The depth of the diffuse double-layer region is characterized by the Debye length (κ^{-1}), which is directly related to ionic strength of the bulk aqueous solution:

$$\kappa^{-1} = ([\epsilon\epsilon_0 kT/[2n^0 z^2 e^2])^{1/2} \quad (1)$$

where n^0 is the number concentration, z is the absolute charge of the analyte ion, e is the charge on an electron, ϵ is the dielectric constant of the interfacial region, ϵ_0 is the permeativity of free space, k is the Boltzmann constant, and T is the absolute temperature.[1a]

The magnitude of interfacial E fields depends on the concentration of ions and solvent molecules immediately adjacent to metal surface and, consequently, is sensitive to diffuse double-layer structure. In solutions with high ionic strength, the diffuse double-layer region at the electrochemical interface is compressed (small κ^{-1}) and the corresponding interfacial E field is expected to be enormous ($\sim 10^9$ V^{-1} m^{-1}). For large κ^{-1}, i.e., low ionic strength solutions, the interfacial E field is expected to be smaller than the former case, although still quite large.

Previous spectroscopic investigations of electrochemical interfaces have utilized the Stark effect to provide a route to direct measurement of interfacial E fields.[3,5] The vibrational Stark effect can be described as a perturbation of the energy of vibrational transitions due to the presence of an E field; it largely originates from additional anharmonicity that is created within molecular bonds by the presence of an E field, in which the bond is both mechanically and electronically distorted from equilibrium.[6] For dipolar probe molecules at surfaces, a first-order vibrational Stark effect is anticipated for both Raman and IR-active vibrational spectra.[7] Stark tuning is proportionally related to the electric field to which the probe molecule is exposed, as related by the expression for the interaction of a dipole (μ) with an electric field (E), approximated here by a Taylor expansion:

$$\Delta\nu = 1/hc(\Delta\mu E + {}^1/_2 E\Delta\alpha E + ...) \quad (2)$$

10.1021/jp0344693 CCC: $25.00
Published on Web 06/27/2003

Several papers have presented theoretical descriptions of the vibrational Stark effect.[6]

Sensitivity of a vibrational frequency to an *E* field, or Stark tuning rate ($d\nu/dE$), of a probe molecule is used to measure changes in *E* fields to obtain structural information for a diverse range of interfacial systems (e.g., electrochemical interfaces, proteins, zeolites).[3,5,8] Spectroelectrochemical investigations of polarized interfaces obtain Stark tuning rates by inducing large changes in interfacial *E* fields by varying the potential applied to a metal surface. Consequently, the *E* fields reported by this method do not represent an absolute *E* field, but rather the difference (ΔE) between an interfacial *E* field that occurs for one applied potential relative to another.

In this article, vibrational Stark tuning rates of a neutral nitrile group pendant to an alkanethiol are used to detect changes in interfacial *E* field strength due to variation in applied potential. Use of the alkane chain spacer between the thiol anchoring group and the terminal nitrile group is essential to prevent charge-transfer interactions between the probe molecule and the metal surface, which would easily overwhelm the desired response (i.e., purely electrostatic Stark tuning). Alkanethiol bearing nitriles molecules were also co-immobilized with methyl-terminated alkanethiol molecules to form mixed monolayers. This surface arrangement was designed to restrain nitrile orientation, as well as to prevent additional charge-transfer interactions between the probe molecule and the metal surface as a result of reorientation of the mercaptoalkanenitrile. Nitrile was chosen as the pendant group for its large dipole moment ($\sim$3 D)[9] to maximize the interaction between the molecular dipole and applied *E* field.[7] Chidsey and Loiacono performed infrared spectroscopic and electrochemical studies of single-component monolayers composed of nitrile-terminated alkanethiols at Au surfaces, which indicate nearly crystalline packing of the monolayers that demonstrate substantial ability to block electron transfer from solution-phase redox species to the electrode surface.[10]

Direct observation of structure at an electrified SAM/aqueous interface and in situ SAM characterization are challenging analytical measurements due to limitations inherent to spectroscopic detection of a single monolayer. Surface-enhanced Raman scattering (SERS) spectroscopy, which enhances the Raman scattering signal by as much as a factor of 10,[6] has been successfully employed to meet these detection challenges to provide in situ characterization of SAMs and adsorbate surface structure.[11] Previous work in this laboratory[12] has utilized SERS-based spectroelectrochemistry to show that Stark tuning of the stretching vibrational mode of surface-immobilized nitrile groups acts as an interfacial *E* field probe that is sensitive to structural changes within the diffuse double layer. Furthermore, this technique was capable of measuring interfacial *E* fields that are consistent with diffuse double-layer theory. In this article, nitrile-terminated alkanethiols are utilized to characterize diffuse double-layer structure as a function of distance from the electrode surface: the Stark tuning rate associated with the nitrile stretching mode of the pendant nitrile is employed as a localized probe of interfacial *E* fields within the diffuse double-layer region: the spatial position of the nitrile species relative to the diffuse double layer is manipulated by varying the alkane chain lengths of the diluent alkanethiol species (Scheme 1).

The use of the methyl terminus of the diluent alkanethiol to establish the interfacial boundary between the monolayer film and the aqueous phase is the crux of this experiment. Variation of the molecular probe moiety with respect to the diffuse double layer, which is established by the SAM/solution interface, is

SCHEME 1: Graphical Depiction of the Interfacial Boundary Region for Each Mixed-Monolayer System Investigated in This Study

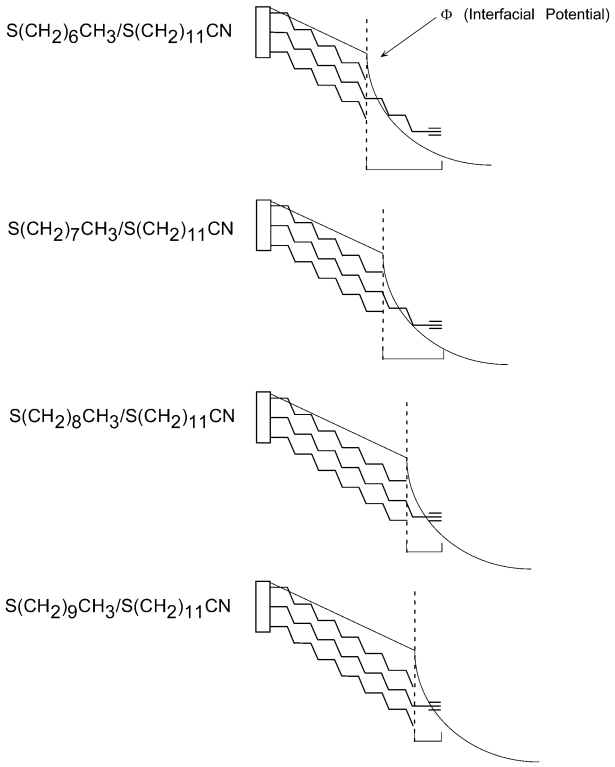

modified by adjusting chain length of the diluent species. Changes in Stark tuning rates are examined as a function of diluent alkane chain length, and the results are used to gain qualitative insight into the structure of the diffuse double layer. A well-defined interfacial boundary region is critical to this experiment and, accordingly, the structure associated with these mixed-monolayer systems must be discussed. SAM composition and conformational order of each mixed-monolayer surface determines the local environment surrounding the probe molecule and, hence, may modulate the probe's response to interfacial *E* fields within the diffuse double layer. For instance, the relative composition of the mixed SAM is expected to affect the apparent location of the SAM terminus. Mixed monolayers with increasing concentrations of the nitrile-bearing thiol species will result in monolayers where nitrile probes are surrounded by other nitrile groups. In this case, the Stark-tuning signal would be equivalent to that obtained from single-component $-S(CH_2)_{11}CN$ monolayers. Here, the nitrile reporter group is effectively isolated from the aqueous interface and cannot be sensitive to structural changes within the diffuse double layer. The molecular conformations of these mixed monolayers are also important: gauche defects may allow analyte ions to penetrate into the monolayer, thereby disrupting the location of the interfacial boundary and destroying the ability to confine the beginning of the diffuse double layer to the SAM/solution interface.

Recent work in this laboratory[13] was performed to investigate the monolayer structure of $HS(CH_2)_{11}CN/HS(CH_2)_6CH_3$ mixed monolayers as a function of their relative composition. Results from these in-situ SERS-based spectroelectrochemical measurements show that Stark tuning rates of pendant nitrile groups depend on monolayer composition, an effect that can be eliminated with sufficient dilution of the nitrile-bearing thiol. This study also demonstrated the use of SERS-based spectroelectrochemistry to monitor relative surface composition: the

TABLE 1: Description of Mixed Monolayers Investigated in This Study and the Composition the Ethanolic Solution from Which Each Monolayer Type Was Assembled

mixed-monolayer type	assembly solution composition
$-S(CH_2)_{10}CH_3/-S(CH_2)_{11}CN$	1:1
$-S(CH_2)_9CH_3/-S(CH_2)_{11}CN$	2:1
$-S(CH_2)_8CH_3/-S(CH_2)_{11}CN$	3:1
$-S(CH_2)_7CH_3/-S(CH_2)_{11}CN$	4:1
$-S(CH_2)_6CH_3/-S(CH_2)_{11}CN$	6:1

ratio of SERS intensities of vibrational modes associated with the two distinct terminal groups (methyl and nitrile) served as a parameter through which surface composition can be determined and controlled.

In this work, the dependence of the Stark tuning rate of the nitrile stretching frequency will be examined as a function of the alkane chain length of the diluent thiol (Scheme 1), as well as a function of ionic strength. SERS spectra will be used to monitor surface coverage of the nitrile terminal groups associated with each mixed monolayer for the purpose of controlling the effects of composition on the Stark-tuning probe. Results will be used to characterize the environment of electrified self-assembled monolayer/aqueous solution interfaces on a sub-nanometer distance scale.

Experimental Section

Substrate Preparation. Electrodes were constructed from 99.999% Ag rod (7 mm diameter, Alfa Aesar). All Ag surfaces were polished with 800, 1500, and 2000 grit silicon carbide paper (3M), followed by successive polishing stages with silica polishing particle slurries on microfiber polishing cloth (Buehler). Ag surfaces were polished down to 0.05 μm roughness. Surfaces were sonicated in ethanol for 15 min to facilitate removal of the remaining silica.

SAM Preparation. Heptanethiol (98%), octanethiol (97%), nonanethiol (98%), decanethiol (98%), and undecanethiol (98%) were used as received from Sigma-Aldrich. 12-Mercaptododecanethiol was synthesized according to a published procedure.[13,14] Mixed monolayers were assembled from ethanolic solutions composed of a given ratio of 10 mM alkanethiol ($HS(CH_2)_xCH_3$) to 10 mM 12-mercaptododecanenitrile ($HS(CH_2)_{11}CN$); see Table 1. The ratio of $(HS(CH_2)_xCH_3)$:$(HS(CH_2)_{11}CN)$ in ethanolic solution was adjusted for each mixed-monolayer system to compensate for the preferential adsorption of longer chain alkanethiols to maintain constant surface coverage of the pendant nitrile for all mixed-SAM surfaces.

Spectroelectrochemical Measurements. A Pine RDE4 potentiostat was used to control the applied potential in a three-electrode configuration. All measurements were referenced to a Ag/AgCl (saturated KCl) electrode and platinum wire was employed as the counter-electrode. Excitation radiation at 514 nm was provided by a Lexel 95 Ar^+ laser. The excitation beam was brought to a focus with a modest energy density of 70 mW/cm^2 at the sample surface. The p-polarized excitation beam was fixed at an incident angle of 55°, in the $y-z$ plane, with respect to the surface normal, z, and scattered light was collected at 60° in the $x-z$ plane with an f/1.4 camera lens (JML Optics). The elastically scattered light was filtered from the signal with a holographic notch filter (Kaiser) before being focused with a second f/1.4 camera lens onto a fiber optic bundle. The fiber optic cable, composed of 100 μm low hydroxyl quartz fibers, was constructed in a spot-to-line configuration: The collected light was brought to a focus at the circular fiber optic head and transmitted to a fiber optic line output. The resulting line-shaped signal was refocused at an entrance slit (110 μm) into an F/4 Spex monochromator ($^1/_2$ m focal length). The Raman scattered light was detected by a 265 × 1024 pixel CCD (Andor Technology) thermoelectrically cooled to −70 °C.

TABLE 2: Relative Composition of Each Mixed Monolayer[a]

mixed-monolayer type	$I(\nu(CH_3))/I(\nu(CN))$
$-S(CH_2)_{10}CH_3/-S(CH_2)_{11}CN$	1.9 ± 1.6
$-S(CH_2)_9CH_3/-S(CH_2)_{11}CN$	2.4 ± 0.8
$-S(CH_2)_8CH_3/-S(CH_2)_{11}CN$	1.4 ± 0.5
$-S(CH_2)_7CH_3/-S(CH_2)_{11}CN$	2.1 ± 1.3
$-S(CH_2)_6CH_3/-S(CH_2)_{11}CN$	2.3 ± 0.9

[a] $I(\nu(CH_3))/I(\nu(CN))$ represents the ratio of intensities of the CH_2 stretching mode associated with diluent alkanethiol to that of the nitrile stretching mode.

All spectroelectrochemical measurements were performed on aqueous solutions composed of doubly distilled deionized water (Nanopure) and sodium perchlorate (99.9%, Sigma-Aldrich). Three different concentrations of electrolyte were employed to achieve differing double-layer structure: 10 mM, 100 mM, and 1 M $NaClO_4$ were prepared.

Stark tuning rates were obtained by measuring the peak position of the nitrile stretching mode at varying applied potentials (vs Ag/AgCl). The numerical values of the Stark tuning rates were computed from changes in the peak frequency divided by the differences in applied voltage. The Stark tuning rates associated with all mixed-monolayer surfaces bearing a suitably low surface coverage of the nitrile-terminated thiol were averaged from numerous individual measurements of the Stark tuning rates ($N > 6$). For most cases, the uncertainties were estimated from multiple measurements obtained from several separately prepared silver surfaces ($N > 3$).

Results and Discussion

Monolayer Composition and Conformational Order. The relative composition of each type of mixed monolayer was scrutinized to ensure that the relative surface coverage of the nitrile did not vary significantly between samples. The ratio of the SERS intensity of the nitrile stretching mode (~2250 cm^{-1}) versus the vibrational mode associated with the methyl group (2873 cm^{-1}) has been shown to be sensitive to the relative surface coverage of the SAMs.[13] Accordingly, $I_{\nu(CN)}/I_{\nu(CH_3)}$ was used to characterize surface coverage of the nitrile group for all mixed-SAM surfaces used in these experiments.

The numerical values of $I_{\nu(CN)}/I_{\nu(CH_3)}$ were computed for all data at a constant applied potential. Stark tuning data, associated with $I_{\nu(CN)}/I_{\nu(CH_3)}$ values that deviated significantly from average values (greater than a factor of 2) observed for the entire series of mixed SAMs, were discarded. Differences in the measured $I_{\nu(CN)}/I_{\nu(CH_3)}$ between the mixed SAMs are not statistically significant; see Table 2.

The conformational structure associated with each mixed-monolayer composition was examined to assess the relative disorder associated with each type of mixed monolayer. The C−H stretching region of SERS spectra presents an ideal route to conformational characterization of mixed SAMs: it is easily accessible and rich in structural information.[15] Figure 1 depicts the C−H stretching region for each mixed-monolayer type. The vibrational band that appears at 2813 cm^{-1} is attributed to $\nu(CH_2)$ vibrations associated with gauche defects, which indicates that these mixed SAMs are somewhat disordered.[13] In these experiments, the band located at 2813 cm^{-1} is only observed after excursions to positive potentials (>+0.2 V vs Ag/AgCl), which are induced to boost SERS signal. This procedure is required to have sufficient SERS signal to detect

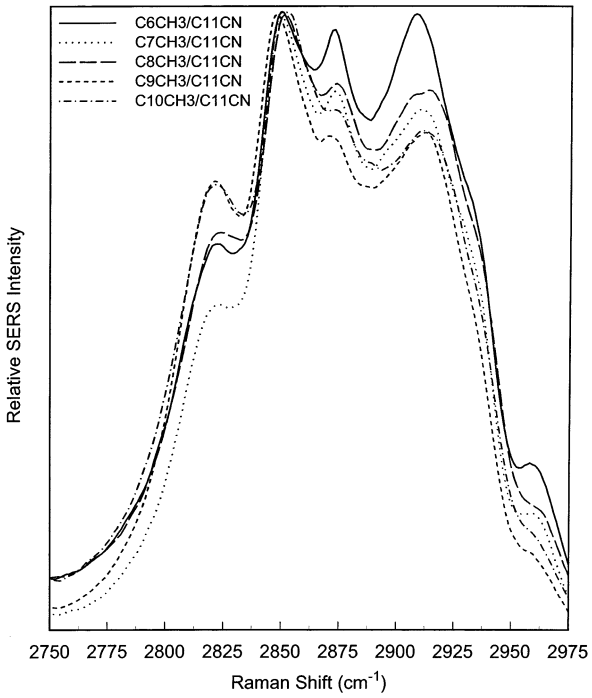

Figure 1. SERS spectra for the C−H stretching region for each mixed-monolayer type.

mixed SAMs in situ. Positive potentials are known to induce surface roughening of the Ag surface, which, in turn, has been shown to result in the development of gauche defects of the SAM film and concomitant monolayer disorder.[16] It is surprising that the Stark effect is still observed upon substantial gauche defect formation. Formation of gauche defects was expected to be accompanied by significant penetration of ions into the monolayer and subsequent rearrangement of diffuse double-layer structure. The data suggest, however, that the appearance of gauche defects within the monolayer is not accompanied by significant rearrangement (i.e., compression) of diffuse double-layer structure.

Observed Vibrational Stark Effect. Figure 2 illustrates the Stark effect exhibited by the nitrile stretching vibrational frequency associated with each mixed-monolayer film: the nitrile stretching frequency increases with increasingly positive applied potential. As previously reported, the direction of the tuning response is consistent with the behavior of Ag surfaces, where the potential of zero charge (∼−0.9 V (vs Ag/AgCl)),[11h,17] requires that, for most applied potentials visited during the experiment, the metallic surface be positively charged. Consequently, external *E* fields associated with a positively charged metal surface oppose that of the permanent dipole moment of the immobilized nitrile species. As a result, the stretching frequency of the nitrile bond increases because the *E* field acts to compress the nitrile bond, which in turn creates a steeper potential well and, subsequently, higher energy vibrational transitions with increasingly positive applied potentials.[12] Furthermore, the peak position of pendant nitrile groups immobilized in mixed SAMs, measured at applied potentials near the potential of zero charge (−0.9 V vs Ag/AgCl), approaches that of nitrile stretching mode of neat 12-mercaptododecanenitrile, 2247 cm^{-1}.[18] This latter observation also serves as further evidence that our description of this interfacial system is correct: the direction of measured Stark tuning rates is consistent with Scheme 1, where the methylene chain of the probe molecule projects beyond the terminus established by the diluent alkanethiols and the nitrile probe is positioned such that

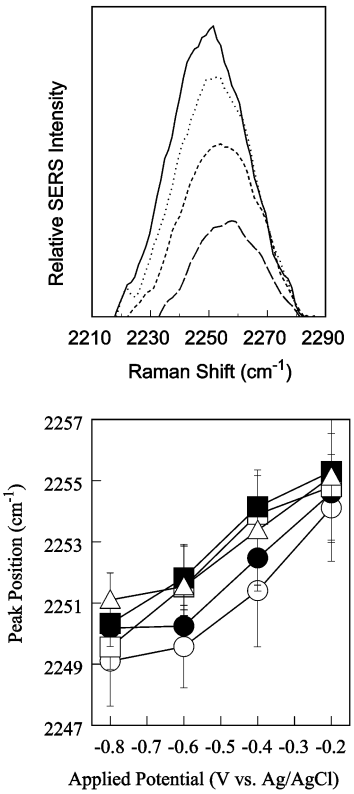

Figure 2. Top panel: nitrile stretching region of SERS spectra: $C_{11}/C_{11}CN$ SAM as a function of applied potential in 10 mM $NaClO_4$. Bottom panel: Peak position of the nitrile stretching mode due for all mixed-monolayer types in 10 mM $NaClO_4$: $-S(CH_2)_6CH_3/-S(CH_2)_{11}CN$ (○), $-S(CH_2)_7CH_3/-S(CH_2)_{11}CN$ (●), $-S(CH_2)_8CH_3/-S(CH_2)_{11}CN$ (□), $-S(CH_2)_9CH_3/-S(CH_2)_{11}CN$ (■), $-S(CH_2)_{10}CH_3/-S(CH_2)_{11}CN$ (▲).

its internal electric dipole moment opposes that of the external electric field.

The SERS intensity of the nitrile mode also exhibits a reversible potential dependence, in which the intensity decreases upon application of increasingly positive applied potentials. Two mechanisms could explain the observed behavior: First, surface selection rules of the conductive substrate could reflect a change in the orientation of the adsorbate as a function of applied potential, where the alkane chain of the probe molecule reorients to align the dipole of the nitrile relative to the applied interfacial *E* field. Our data do not support this mechanism: previous research on the $-S(CH_2)_6CH_3/-S(CH_2)_{11}CN$ SAM system shows that the intensities of C−H and C−S stretching modes from gauche defects decrease as the applied potential becomes increasingly positive.[13] These data are contrary to the postulated reorientation mechanism, in which one would expect to see increasing disorder at more positive applied potentials, where mercaptododecanenitrile molecules experience the greatest driving force to adopt more gauche defects to reorient the dipole of the pendant nitrile with respect to the applied field. Further evidence supporting the integrity of the probe molecule conformation can be seen in Figure 2 (bottom), where the Stark tuning rate (i.e., slope of the bottom plot) does not decrease or change sign for increasingly positive applied potential. Potential-dependent reorientation of the nitrile bond would change the effective field experienced by the nitrile dipole: the electrostatic torque exerted by the *E* field on the dipole would cause the dipole to align with the *E* field and, accordingly, cause the Stark tuning rates of the nitrile stretching mode to become smaller or reverse direction. These results further indicate that the longer chain mercaptoalkanenitrile adopts an extended conformation

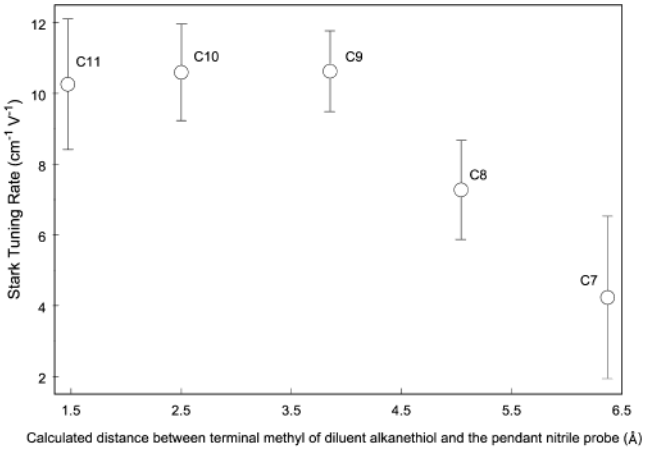

Figure 3. Spatial profile of nitrile Stark tuning rates in 1 M $NaClO_4$: Stark tuning rates of each nitrile probe associated with each different mixed monolayer. Each SAM is characterized by the number of carbons in the diluent chain, which serves as an indicator of the relative position of the nitrile group. The corresponding distance between the nitrile probe and the methyl terminus of the diluent alkanethiol was estimated from geometric optimizations (HF/6-311G(d,p)) of the electronic structure of the mercaprododecanenitrile and each diluent alknaethiol.

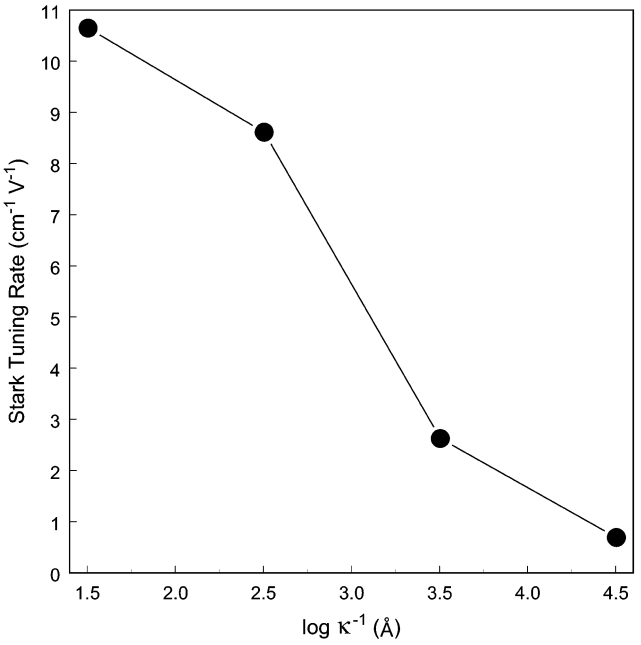

Figure 4. Measured Stark tuning rates for $-S(CH_2)_{10}CH_3/-S(CH_2)_{11}CN$ mixed monolayers as a function of increasing Debye lengths (or decreasing ionic strengths).

beyond the methyl terminus established by the shorter diluent alkanethiol regardless of the applied field. This latter observation suggests that the energy associated with interactions of the pendant polar nitrile species with the solvent dominate over other interfacial forces (e.g., van der Waals interactions, hydrophobic effects) that would lead to reorientation of the terminal nitrile group relative to the plane of the interface.

An alternative explanation of the potential-dependent change in the SERS intensity is that the applied potential sufficiently perturbs the surface-plasmon polaritons, which are responsible for the electromagnetic component of the surface enhancement, so that the Ag surface loses some of its SERS activity within a given applied potential region. Mulvaney et al. report significant but reversible changes in both the position and shape of the electronic absorption spectra of Ag colloidal films at electrode surfaces upon application of applied potential.[19] Accordingly, it is possible that at more positive potentials, the surface plasmon polaritons shift to a different energy that is less resonant with the incoming excitation radiation, thereby resulting in a loss of surface-enhancement.

Spatial Profile of Stark Tuning Rates. The SERS-based spectroelectrochemical results indicate that the Stark tuning rates of pendant nitriles are sensitive to the position of the probe relative to the SAM/solution interface. The effective *E* field experienced by the nitrile group depends on the length of the alkane chain of the surrounding alkanethiol; see Figure 3. As the diluent chain length becomes shorter and the nitrile probe penetrates more deeply into the diffuse double layer, the reporter group experiences diminishing *E* fields. This trend is consistent with double-layer theory, which predicts that for these conditions the *E* field decays on the scale of the Debye length, ~3 Å, such that the diffuse double-layer region ends before it reaches the position of the nitrile group. Further evidence in support of this interpretation can be found in Figure 4, where the response of the nitrile probes placed in a very low-ionic strength solutions are reported. Results indicate that the Stark tuning rates for this situation are vanishingly small due to the slow decay of the interface potential corresponding to negligible *E* fields.

The data presented in Figure 3 show that the interfacial *E* field decays with increasing distance from the interfacial boundary. However, the measured interfacial *E* field still persists even though the probe extends beyond the terminus of the diluent chain by ~6 Å, a distance that was determined with ab initio electronic structure calculations of $-S(CH_2)_{11}CN$ and $-S(CH_2)_6CH_3$ (HF/6-311G(d,p)). The observed diffuse double-layer region, which is substantially longer than the predicted Debye length (~3 Å), is attributed to the finite size of the ions within the double layer (the hydrated ionic radii of sodium and perchlorate ions are 4.5 and 3.5 Å, respectively).[20] Also, the apparently slow decay of interfacial *E* fields inside the double layer is also consistent with the theory of Lum, Chandler, and Weeks, who predict that the interaction of hydrophobic surfaces with water results in a lowering of the water density immediately adjacent to the interface.[21] It is reasonable to assume that the local concentration of ions within a lower density aqueous region is smaller than would be predicted for bulk water; this would further slow the decay of the *E* field near the interface compared to a homogeneous Gouy−Chapman model for the double layer.

Effect of Debye Length on the Observed Interfacial *E*-Field Profile. Figure 5 illustrates the effect of ionic strength on interfacial *E* fields measured by the nitrile probe as a function of its relative position from the alkane/solution interface. Here, the Stark tuning rate associated with each mixed-monolayer system (e.g., $-S(CH_2)_6CH_3/-S(CH_2)_{11}CN$) is used to spatially map a region of the diffuse double-layer region as a function Debye length. The Stark tuning rates exhibited by each probe are dependent on both probe position and ionic strength. For instance, nitrile groups that are positioned closest to the interfacial boundary, represented by $-S(CH_2)_{10}CH_3/-S(CH_2)_{11}CN$ and $-S(CH_2)_9CH_3/-S(CH_2)_{11}CN$, are exposed to the highest *E* fields and generally exhibit the largest tuning rates regardless of ionic strength. In contrast, nitrile probes immobilized within $-S(CH_2)_6CH_3/-S(CH_2)_{11}CN$ SAMs, where the probe is placed the deepest into the diffuse double layer and furthest from the metal surface, experience weaker interfacial *E* fields and Stark tuning rates associated with these nitrile probes are smaller. Nitrile groups that are placed between either of these extremes follow similar trends, in which the distance from the interfacial boundary is, in general, inversely proportional to the measured tuning rates.

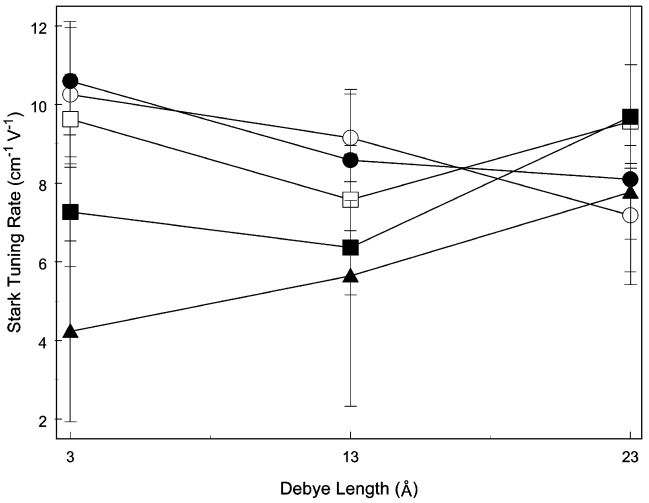

Figure 5. Spatial profile of nitrile Stark tuning rates in as a function of Debye length (κ^{-1}): $-S(CH_2)_{10}CH_3/-S(CH_2)_{11}CN$ (○), $-S(CH_2)_9CH_3/-S(CH_2)_{11}CN$ (●), $-S(CH_2)_8CH_3/-S(CH_2)_{11}CN$ (□), $-S(CH_2)_7CH_3/-S(CH_2)_{11}CN$ (■), $-S(CH_2)_6CH_3/-S(CH_2)_{11}CN$ (▲).

It is also instructive to examine the distribution of the tuning rates simply as a function of Debye length. For the longest Debye length, where interfacial *E* fields are anticipated to be similar for all probe positions, the Stark tuning rates associated with each probe location are statistically indistinguishable. The intermediate Debye length shows that although the Stark tuning rates are essentially the same, they begin to diverge. The shortest Debye length displays the sharpest divergence, in which the Stark tuning rates reveal stronger changes in the interfacial environments.

Further examination of the behavior of each individual mixed-monolayer systems reveals another trend consistent with Gouy−Chapman theory. Pendant nitrile groups arising from monolayer systems for which the probe moiety is located very close to the interfacial boundary, $-S(CH_2)_{10}CH_3/-S(CH_2)_{11}CN$ and $-S(CH_2)_9CH_3/-S(CH_2)_{11}CN$, exhibit increasing interfacial *E* fields as the Debye length becomes shorter. Again, this trend is consistent with expectations, in which very compact Debye lengths produce the largest potential gradients but only in spatial regions located within few ångstroms of the interfacial boundary. In contrast, nitrile probe species associated with the other mixed-monolayer systems, in which the nitrile group is located progressively farther from the interfacial boundary, the Stark tuning rates do not increase upon exposure to increasingly more compact diffuse double-layer regions: Stark tuning rates exhibited by nitrile probes associated with $-S(CH_2)_8CH_3/-S(CH_2)_{11}CN$ and $-S(CH_2)_7CH_3/-S(CH_2)_{11}CN$, intermediate probe positions, do not appear to significantly change, whereas Stark tuning rates associated with the $-S(CH_2)_6CH_3/-S(CH_2)_{11}CN$ exhibit a pronounced decay.

Conclusions

This article describes the use of an in-situ SERS-based spectroelectrochemical method for investigation of spatial structure of the diffuse double layer at a SAM/aqueous solution interface. This spectroelectrochemical method for detection of double-layer structure relies on use of the Stark effect as a local probe of interfacial electric fields, which, in turn, are known to be sensitive to diffuse double-layer structure. In these experiments, high spatial sensitivity is achieved through the use of mixed monolayers composed of $HS(CH_2)_{11}CN$ and $HS(CH_2)_xCH_3$ (where $6 < x < 10$). Stark tuning rates of the SERS-enhanced nitrile stretching mode associated with mixed monolayers composed of $HS(CH_2)_{11}CN$ and $HS(CH_2)_xCH_3$ (where $6 < x < 10$) were used to measure interfacial *E* fields. The straight-chain alkanethiols act as diluent molecules, which establish the boundary between the terminus of the SAM and the beginning of the diffuse double-layer region.

General trends in the experimental data are largely consistent with Gouy−Chapman theory, in which charge density (and resultant large interfacial electric field) depends both on the distance of the probe from the electrode surface and on the Debye length associated with the ionic strength of the aqueous solution phase. Results show that Stark tuning rates associated with nitrile groups located directly adjacent to the SAM/aqueous interface demonstrated the largest magnitudes and experienced limited increases with increasing ionic strength. In constrast, nitrile groups positioned deep inside the diffuse double-layer region exhibited much smaller Stark tuning rates, which reflected the largest changes within the diffuse double layer as a function of ionic strength. At the highest ionic strengths, however, the experimental results indicate that the diffuse double-layer region is longer than that predicted by Gouy−Chapman theory. This observation is attributed to the finite size of the ions that comprise the double layer and is also consistent with the possible presence of a lower density water region between the terminus of the hydrophobic SAM and bulk solution, which could also contribute to the diffuse double layer extending further into solution. These results also demonstrate that a nitrile-terminated alkanethiol diluted into mixed SAMs containing shorter alkanethiols protrude well beyond the methyl terminus established by the shorter diluent alkanethiol. This latter observation suggests that the energetics associated with solvation of the pendant highly polar nitrile species dominates the van der Waals/hydrophobic forces that might compel the extended methylene chain to change conformation (or collapse) to maximize the interaction with the underlying methyl termini. In summary, this paper demonstrates the use of SERS-based spectroelectrochemical measurements to provide spatially resolved, in situ characterization (on the order of ångstroms) of diffuse double-layer structure at SAM-modified electrochemical interfaces.

Acknowledgment. This work would not have been possible without instruction from Dominic Tiani and Jeanne Pemberton on the art of Ag electrode polishing. We also thank Henry S. White for helpful discussions on diffuse double-layer structure. An allocation of computer time from the Center for High Performance Computing at the University of Utah is gratefully acknowledged. This research was supported by the Department of Energy under Grant DE-FG03-93ER14333.

Note Added after ASAP Posting. This paper was originally published ASAP on 6/27/2003 before author corrections were received. The corrected version was reposted on 7/8/2003.

References and Notes

(1) (a) *Electrochemical Methods*; Bard, A. J., Faulkner, L. R., Eds.; Wiley and Sons: New York, 1980. (b) Smith, C. P.; White, H. S. *Anal. Chem.* **1992**, *64*, 2398. (c) Glosli, J. N.; Philpott, M. R. *Electrochim. Acta* **1996**, *41*, 2145.

(2) Bard, A. J.; Abrũna, H. D.; Chidsey, C. E.; Faulkner, L. R.; Feldberg, S. E.; Itaya, K.; Majda, M.; Melroy, O.; Murray, R. W.; Porter, M. D.; Soriaga, M. P.; White, H. S. *J. Phys. Chem.* **1993**, *97*, 7147.

(3) (a) Hanken, D. G.; Corn, R. M. *Anal. Chem.* **1997**, *69*, 3665. (b) Korzeniewski, C.; Shirts, R. B.; Pons, S. *J. Phys. Chem.* **1985**, *89*, 2297. (c) Korzeniewski, C.; Pons, S. *J. Vac. Sci. Technol. B* **1985**, *3*, 1421. (d) Korzeniewski, C.; Pons, S.; Schmidt, P. P.; Severson, M. W. *J. Chem. Phys.* **1986**, *85*, 4153. (e) Pope, J. M.; Zheng, T.; Kimbrell, S.; Buttry, D. A. *J. Am. Chem. Soc.* **1992**, *114*, 10085. (f) Pope, J. M.; Buttry, D. A. *J. Electroanal. Chem.* **2001**, *498*, 75.

(4) (a) Fan, F.-R. F.; Bard, A. J. *J. Am. Chem. Soc.* **1987**, *109*, 6262. (b) Smith, C. P.; Maeda, M.; Atanososka, L.; White, H. S.; McClure, D. J. *J. Phys. Chem.* **1988**, *92*, 199. (c) Parker, J. L.; Christenson, H. K. *J. Chem. Phys.* **1988**, *88*, 8013. (d) Hillier, A. C.; Kim, S.; Bard, A. J. *J. Phys. Chem.* **1996**, *100*, 18808. (e) Hu, K.; Fan, F.-R.; Bard, A. J.; Hillier, A. C. *J. Phys. Chem. B* **1997**, *101*, 8298.

(5) Lambert, D. K. *J. Chem. Phys.* **1988**, *89*, 3847.

(6) (a) Boxer; et al. *J. Phys. Chem. A* **2002**, *106*, 469. (b) Bishop, D. M. *J. Chem. Phys.* **1993**, *98*, 3179. (c) Hush, N. S.; Reimers, J. R. *J. Phys. Chem.* **1995**, *99*, 15798 and (d) Lambert, D. K. *Solid State Commun.* **1984**, *51*, 297.

(7) Condon, E. U. *Phys. Rev.* **1932**, *41*, 759.

(8) (a)Kao, W. Y.; Davis, C. E.; Kim, Y. I.; Beach, J. M. *Biophys. J.* **2001**, *81*, 1163. (b) Loew, L. M.; Simpson, L. M. *Biophys. J.* **1981**, *34*, 353. (c) Park, E. S.; Thomas, M. R.; Boxer, S. G. *J. Am. Chem. Soc.* **2000**, *122*, 12297. (d) Park, E. S.; Andrews, S. S.; Hu, R. B.; Boxer, S. G. *J. Phys. Chem. B* **1999**, *103*, 9813. (e) Boxer, S. G. Stark spectroscopy: applications in chemistry, biology, and materials science. *Ann. Rev. Phys. Chem.* **1997**, *48*, 213C. (f) Xiang, P. L.; Grassian, V. H.; Larsen, S. C. *J. Phys. Chem. B* **1999**, *103*, 5058.]

(9) *Landolt-Boernstein, Numerical Data and Functional Relationships in Science and Technology*; Hellwege, K. H.; Springer-Verlag: Heidelberg, 1982; Group II, Vol. 14 (a).

(10) Chidesy, C. E. D.; Loiacono, D. N. *Langmuir* **1990**, *6*, 682.

(11) (a) Taylor, C. E.; Schoenfisch, M. H.; Pemberton, J. E. *Langmuir* **2000**, *16*, 2902. (b) Taylor, C. E.; Garvey, S. D.; Pemberton, J. E. *Anal. Chem.* **1996**, *68*, 2401. (c) Schoenfisch, M. H.; Ross, A. M.; Pemberton, J. E. *Langmuir* **2000**, *16*, 2907. (d) Thomas, B.; Doubova, L.; Stoicoviciu, L.; Trasatti, S. *J. Electroanal. Chem.* **1988**, *244*, 133. (e) Campion, A.; Hallmark, V. *Chem. Phys. Lett.* **1984**, *110*, 561. (f) Hubbard, A.; Salaita, G.; Lu, F.; Laguren-Davidson, L. *Langmuir* **1988**, *4*, 224. (g) Hamelin, A.; Valette, G. *J. Electroanal. Chem.* **1973**, *45*, 301. (h) Weaver, M. J.; Larkin, D.; Guyer, K.; Hupp, J. *J. Electroanal. Chem.* **1982**, *138*, 401.

(12) Oklejas, V.; Sjostrom, C.; Harris, J. M. *J. Am. Chem. Soc.* **2002**, *124*, 2408.

(13) Oklejas, V.; Harris, J. M. *Langmuir* **2003**, *19*, 5794.

(14) Bain, C. D.; Troughton, E. B.; Tao, Y. T.; Evall, J.; Whitesides, G. M.; Nuzzo, R. G. *J. Am. Chem. Soc.* **1989**, *111*, 321. (Supporting Information).

(15) [(a) Snyder, R. G.; Strauss, H. L.; Elliger, C. A. *J. Phys. Chem.* **1982**, *86*, 5145. (b) Hill, I. R.; Levin, I. W. *J. Phys. Chem.* **1979**, *70*, 842. (c) Larsson, K.; Rand, R. P. *Biochim. Biophys. Acta* **1973**, *326*, 245. (d) Orendorff, C. J.; Ducey, M. W., Jr.; Pemberton, J. E. *J. Phys. Chem. A*, in press.

(16) Bryant, M. A.; Pemberton, J. E. *J. Am. Chem. Soc.* **1991**, *113*, 8284

(17) (a) Schoenfisch, M. H.; Pemberton, J. E. *Langmuir* **1999**, *15*, 509. (b) Larkin, D.; Guyer, K. L.; Hupp, J. T.; Weaver, M. J. *J. Electroanal. Chem.* **1982**, *138*, 401.

(18) Oklejas, V.; Harris, J. Unpublished results.

(19) **[**19] Ung, T.; Giersig, M.; Dunstan, D.; Mulvaney, P. *Langmuir* **1997**, *13*, 1773.

(20) Kielland, J. *J. Am. Chem. Soc.* **1937**, *59*, 1675.

(21) Lum, K.; Chandler, D.; Weeks, J. D. *J. Phys. Chem. B* **1999**, *103*, 4570.